High Order Workshop: computations performed with JAGUAR, an in-house CFD code based on a Spectral Difference formalism

N. Villedieu, G. Puigt and J-F. Boussuge
CERFACS, 42 avenue de Coriolis 31057 Toulouse

Correspondance author: N. Villedieu, villedie@cerfacs.fr

1 Introduction

Spectral Difference (SD) method was first developed by Liu *et al.* [4] for conservative laws on unstructured grids and then extended to Euler equations by Wang *et al.* [8]. Lastly, this method has been applied to a broad range of different applications such as aero-acoustic [2,7] and aero-elasticity [5, 6]. This method is very similar to Discontinuous Galerkin (DG) and Spectral Volume (SV) methods in the sense that they share the same solution space, i.e., the space of piecewise discontinuous polynomials, and some Riemann solvers are used at the element interfaces to provide solution coupling between the discontinuous elements and appropriate numerical dissipation necessary to achieve stability. In addition, all of them are conservative at the element level, making them suitable for problems with discontinuities. They differ on how solution unknowns or Degrees of Freedom (DoFs) are chosen, and how the DoFs are updated. In a DG method, the DoFs are either the expansion coefficients for a given set of polynomial basis functions or solutions at selected locations within the element. In a SV method, the DoFs are sub-cell averaged solutions, while in the SD method, the DoFs are the solutions at (usually) the quadrature points. The difference between the DG, SV, and SD methods is similar to the difference between the Galerkin Finite Element (FE), Finite Volume (FV), and Finite Difference (FD) methods. The SD method has also been compared with DG and SV in the literature. SD method is known to diminish the number of operations per DoF and to use an easier mathematical formalism than DG. SV main default is associated with the dependence of stability with element subdivisions, something that has non sense in SD.

All these methods have been designed in order to tackle efficiently high order discretization. Indeed, they offer a good alternative to the classical high order techniques which generally consider a single DoF per element or mesh node and for which highly accurate schemes need (very) large stencils. The advantages of the Spectral Difference formalism are the following:

- The procedure inside each volume uses a very simple finite difference formalism and its implementation is (quite) easy.
- Deriving equations accurately, one finds easily that SD does not need complex closure coefficients computation, which is clearly positive since it is a way to diminish any po-

tential problem for industrial computations with distorted grids. This is due to the fact that the differential form of the equations are considered.

The first section of this abstract is dedicated to the code description. In the second section we show results obtained on the case C1.6

2 Code description

Up to now, our code is able to deal only with elements which are quadrilateral in 2D and hexahedron in 3D. Even though the method has also been developed for simplex elements, the treatment of quadrilaterals and hexahedrons is easier because it just consists in repeating two or three times the 1D methodology which is presented below. The treatment of hanging nodes is under development, which will allow to treat complex geometries.

2.1 The Spectral Difference method

This 1D process is repeated for each direction (to get the divergence of each flux) in 2D and 3D. The Spectral Difference solves the differential form of a conservative law. First, consider a 1D conservative law:

$$\frac{\partial W}{\partial t} + \frac{\partial F(W)}{\partial x} = 0, \quad \forall x \in [a;b]. \tag{1}$$

The domain $[a;b]$ is divided in several segments denoted by S_{phys}. Of course, all segments do not necessarily have the same sizes. Each segment S_{phys} in the physical domain is transformed into a standard unit segment $S_{comp} = [0;1]$ (computational domain). As shown on figure 1, for a chosen order of discretization p, S_{comp} is equipped with $p+1$ solution points (circles) and $p+2$ flux points (triangles). The resulting scheme is then $p+1$-th order accurate. Our implementation is based on a staggered distribution of unknowns and solution points and flux points are never the same. Several ways to place the solution and flux points are described in the literature. Here, the solution points are chosen to be the Gauss points and the flux points are the Legendre-Gauss quadrature points plus the two end points 0 and 1, as suggested by Huynh [3].

Figure 1: Repartition of the solution and flux points for $p = 1$

As it has been suggested, Eq. (1) is solved in the reference segment S_{comp} and it writes:

$$\begin{aligned} &\frac{\partial \tilde{W}}{\partial t} + \frac{\partial \tilde{F}(W)}{\partial \xi} = 0, \\ &\tilde{W} = |J| W, \\ &\tilde{F} = |J|\, J^{-1} F, \end{aligned} \tag{2}$$

where J is the Jacobian of the so-called iso-parametric transformation from S_{comp} to S_{phys} , and $|J|$ its determinant. Then, the procedure is as follows:

1. Extrapolate the solution $\tilde{W}$ from the $p+1$ solution points to the $p+2$ flux points using a Lagrange polynomial reconstruction based on the solution point location
2. Transform $\tilde{W}$ to the physical variables W
3. Compute the flux F in the internal flux points, and transform it to $\tilde{F}$
4. Since data are not continuous at the segment boundaries, it is necessary to solve a Riemann problem to compute the flux $\tilde{F}$ at the flux points located at interfaces between elements
5. When fluxes are computed in each flux point of the S_{comp} domain, compute the $p+1$-th order polynomial passing by every flux point of S_{comp}
6. Differentiate the flux polynomial and evaluate it in all solution points
7. Use the differentiated flux function for computing an increment of the solution in each solution point

Concerning the time integration, several Explicit Runge-Kutta methods are implemented in our code. The best practice seems the use of the optimized six-step Runge-Kutta method of Bogey and Bailly [1] which is widely used in areo-acoustic. This scheme is fourth order accurate for linear problems, third order accurate for non linear systems of equation and by nature, coefficients are chosen to minimize dispersion and dissipation. Moreover, our experience shows that, even if it needs more steps than the classical three- or four-step Runge-Kutta procedures, the CPU time overhead is counterbalanced by a larger authorized time step to maintain stability.

2.2 Parallel capability and High Performance Computation

We will put many efforts on the High Performance Computing capability of our code. It is nowadays parallelized with a classical MPI approach and asynchronous communications. In complement with parallel capabilities, there is an efficient cache coloring procedure since our experience on unstructured solvers has shown the great interest of cache coloring to minimize cache misses.

3 Case summary

3.1 Case C1.6: Vortex transport by a uniform flow

We will provide results for the two configurations at $M = 0.5$ and $M = 0.05$ on the two sets of meshes provided on the website

3.2 Type of cluster used

The results provided in this abstract were done in serial on a parallel computer composed of nodes with two quad core Intel Xeon "Nehalem" 2.66 Ghz and equipped with a 24-Gb memory (see http://www.cerfacs.fr/files/cerfacs/computing/iDataPlex.jpg).

4 Results

First, we consider the convection of a vortex with slow velocity corresponding to $M = 0.05$. Results obtained with $p = 2, 3, 4$ are shown on figure 2. The profile of the higher order scheme ($p = 4$) is very close to the exact solution.

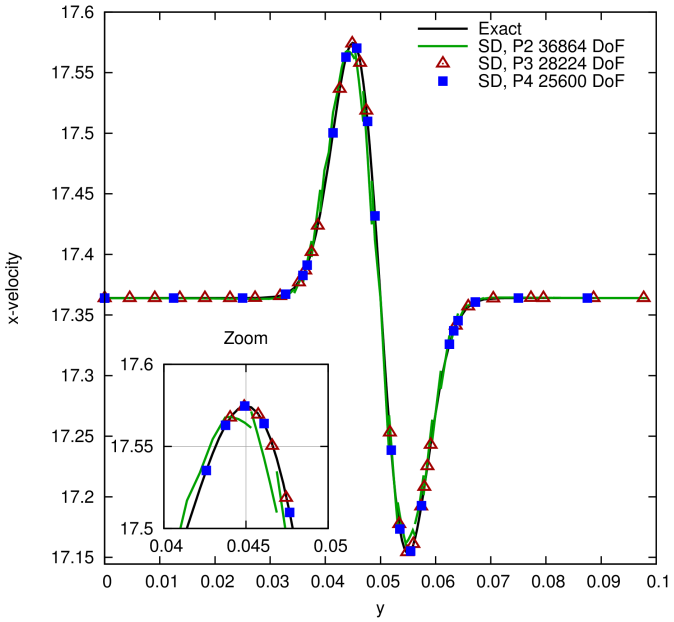

Figure 2: Case $M = 0.05$: x-velocity profile after 50 periods

On figure 3, we can see that the expected order of accuracy is obtained. Moreover, the advantage of the high order scheme is obvious since the 5^{th} order scheme can achieve smallest errors than the other schemes with less degrees of freedom and using a lower CPU time.

Now, we consider the case of the vortex advected at $M = 0.5$ and we analyze the solution after 50 periods (figure 4). We can see again that with $p = 4$ we can get a better solution with less DoF than with $p = 2, 3$.

Fig. 5 presents the solution obtained with $p = 4$ on regular (Cartesian) and irregular grids. Both solutions are in very good agreement.

Finally, it is shown on Fig. 6 that the error analysis recovers the good slope for all orders of accuracy considered in this paper.

5 Conclusion

The results show that the 5^{th} order scheme is a really good candidate to transport small perturbations on long distances such as asked for acoustics problems. Indeed, it needs less

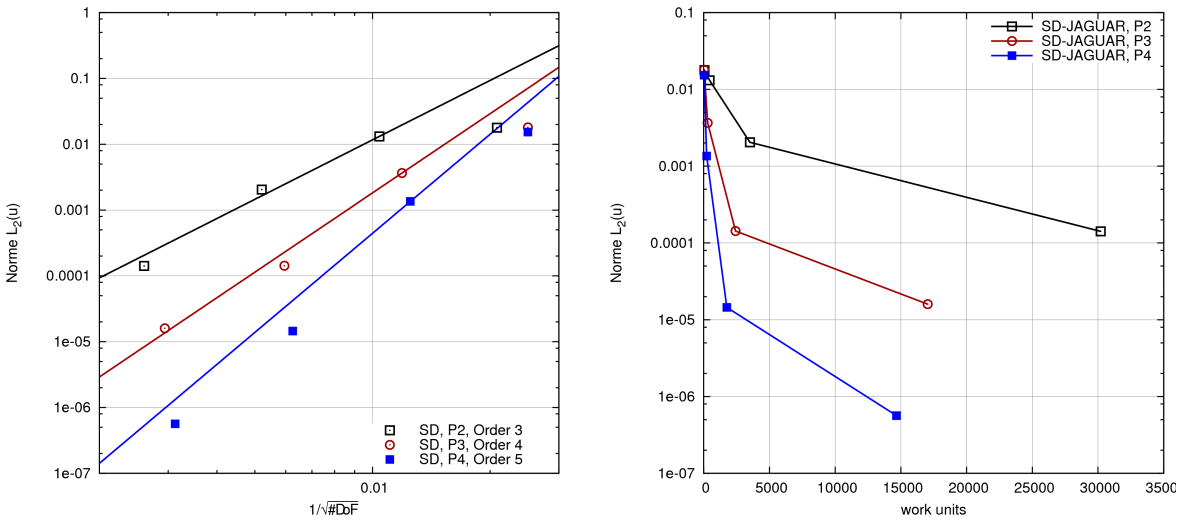

Figure 3: Case $M = 0.05$: grid convergence on the x-velocity profile after 50 periods

CPU time and DoF to achieve a threshold error than low order schemes.

References

[1] C. Bogey and C. Bailly. A family of low dispersive and low dissipative explicit schemes for flow and noise computations. *Journal of Computational Physics*, 194(1), 2004.

[2] K. Van den Abeele. *Development of high-order accurate schemes for unstructured grids*. PhD thesis, Vrije Universiteit Brussel, Department of Mechanical Engineering, 2009.

[3] H. T. Huynh. A Flux Reconstruction approach to high-order schemes including Discontinuous Galerkin methods. In *AIAA Computational Fluid Dynamics Conference*, number AIAA 2007-4079, 2007.

[4] Y. Liu, M. Vinokur, and Z. J. Wang. Spectral difference method for unstructured grids I: Basic formulation. *Journal of Computational Physics*, 216:780–801, 2006.

[5] K. Ou and A. Jameson. On the temporal and spatial accuracy of the spectral difference method on moving deformable grids and the effect of geometry conservation law. In *40th AIAA Fluid Dynamics Conference and Exhibit 28 June - 1 July 2010, Chicago, Illinois*, 2011.

[6] K. Ou and A. Jameson. Towards computational flapping wing aerodynamics of realistic configurations using spectral difference method. In *20th AIAA Computational Fluid Dynamics Conference 27 - 30 June, Honolulu, Hawaii*, 2011.

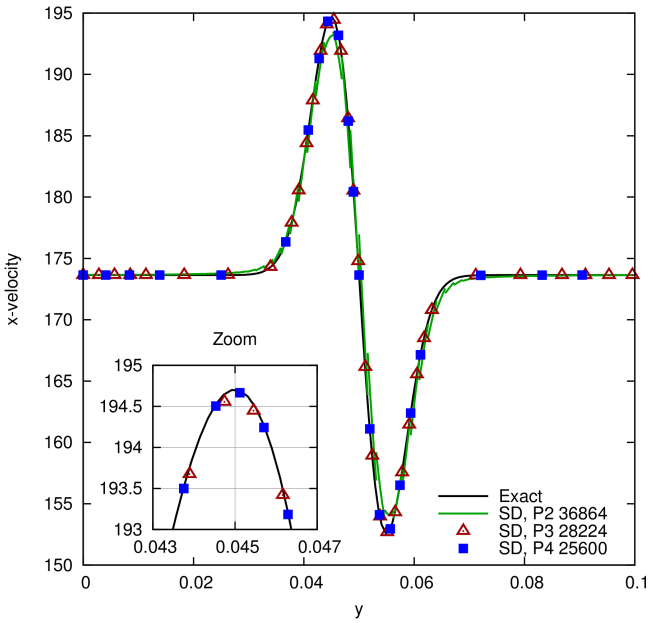

Figure 4: Case $M = 0.5$: x-velocity profile after 50 periods

[7] M. Parsani, G. Ghorbaniasl, and C. Lacor. Validation and application of an high-order spectral difference method for low induced moise simulation. *Journal of Computational Acoustics*, 19(3):241–268, 2011.

[8] Z. J. Wang, Y. Liu, G. May, and A. Jameson. Spectral difference method for unstructured grids II: Extension to the Euler equations. *Journal of Scientific Computing*, 32(1):45–71, 2006.

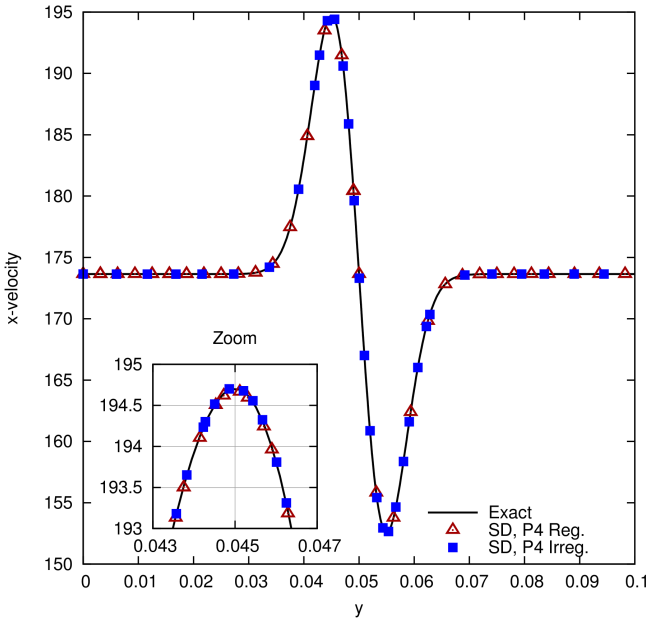

Figure 5: Case $M = 0.5$: x-velocity profile on regular and irregular grids

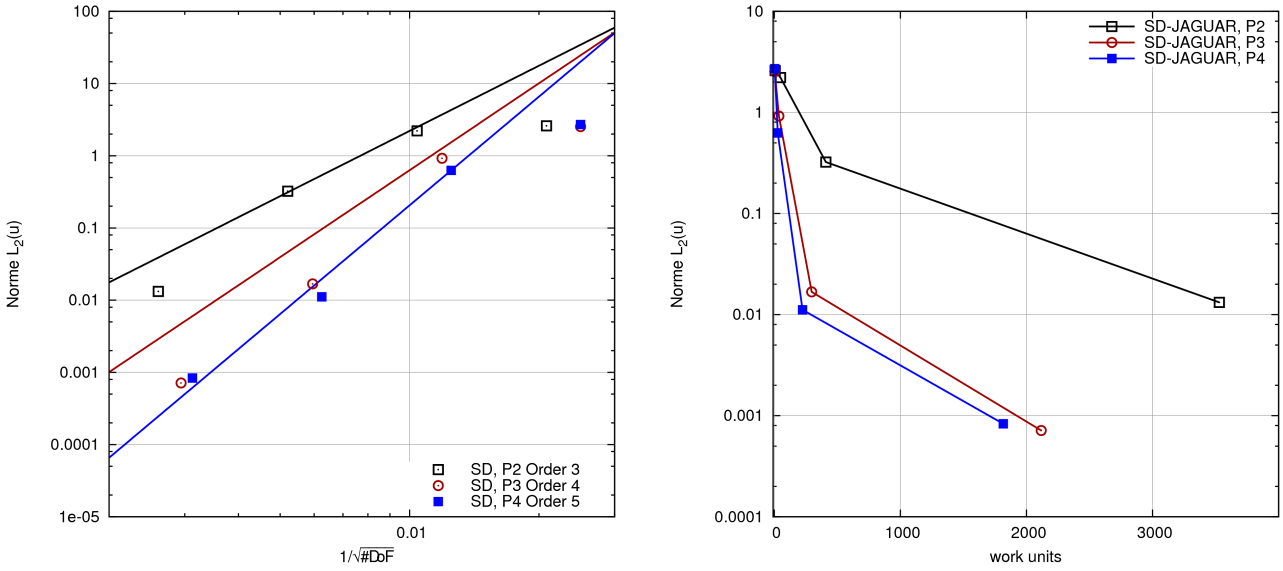

Figure 6: Case $M = 0.5$: grid convergence on the x-velocity profile after 50 periods